# Analyst

# Analyst

# Using the inherent chemistry of the endothelin-1 peptide to develop a rapid assay for pre-transplant donor lung assessment

A. T. Sage,[a] X. Bai,[b,c] M. Cypel,[b,c] M. Liu,[b,c] S. Keshavjee,[b,c] and S. O. Kelley [a,d]

**Endothelin-1 is a potent vasoconstrictive peptide that plays an important role in ex vivo lung perfusion. ET-1 expression levels are predictive of lung transplant outcomes and represent a valuable monitoring tool for surgeons; however, traditional techniques that measure [ET-1] are not suitable for the transplant setting. Herein, we demonstrate a new assay that rapidly measures ET-1 peptide levels in lung perfusate.**

Lung transplantation (LTx) is a life-saving procedure for patients suffering from end-stage lung disease. At present, donor lungs are assessed for transplant suitability based on several physiological parameters including donor/organ medical history and pulmonary compliance measures. These physiological metrics do not reliably predict recipient outcomes after transplant. Thus, the inclusion of lung-specific biomarker tests, prior to transplantation, that could accurately predict LTx outcomes would be of great benefit to patients and transplant teams.

Ex-vivo lung perfusion (EVLP) is a novel technique that has been developed to improve the LTx procedure by affording more time for transplant teams to assess and treat a donor lung under normothermic conditions[1]. As such, EVLP can provide a means by which donor lungs can be treated therapeutically without the detrimental effects of the host immune system[1]. In addition, EVLP can allow for the discovery, validation, and monitoring of predictive biomolecules in EVLP perfusate. In studies using EVLP, circulating levels of the endothelin-1 (ET-1) peptide have been shown to be predictive of donor lung function[2].

ET-1 is an important chemokine that plays a key role in vasoconstriction and fibroblast proliferation[3-5]. The effects of increased ET-1 expression have been implicated as a significant risk factor for both acute and chronic lung injury. Primary graft dysfunction (PGD) is a severe form of acute injury and can occur in approximately 30% of LTx cases. Recent work has demonstrated strong correlation between ET-1 levels and the development of PGD through the disruption of the alveolar-capillary barrier[2]. The profibrotic properties of ET-1 are also a significant contributor to the narrowing of the bronchioles which represents a major characteristic of chronic lung allograft dysfunction (CLAD)[6, 7]. Bronchiolitis obliterans syndrome (BOS) is the predominant form of CLAD and is the principal cause of late graft loss[8]. ET-1 concentrations have been shown to correlate with the development of BOS[9]. Therefore, ET-1 is an extremely powerful biomarker that can be used to predict short- and long-term survival in transplant patients and is a valuable target for molecular diagnostics.

Current detection strategies for ET-1 are based primarily on the enzyme-linked immunosorbent assay (ELISA) protocol[2, 9, 10]. The typical workflow of an ET-1 ELISA can take upwards of 4 hours and requires significant user input. Yet, to be clinically relevant within the decision-making processes of LTx[11], assays must provide sample-to-answer times that are much faster than a typical ELISA. As such, integration of ET-1 testing into the transplant setting remains problematic. Therefore, this work sets out to develop a novel sensing approach for the peptide ET-1. The assay is based on a competitive ELISA-like approach, but incorporates an electrochemical detection method that is sensitive, automatable, and has rapid readout properties.

By exploiting the amino acid sequence of the endothelin-1 peptide, we developed an electrochemical assay to monitor the presence of endogenous ET-1 using an approach similar to that of a competitive ELISA (Figure 1). Using glass microchips (Fig. 1a) with highly structured gold microelectrodes (Fig. 1b), we have previously demonstrated that an electrochemical approach can achieve rapid sample-to-answer times (approximately 30 minutes)[12-14]. As a twenty-one amino acid peptide with an N-terminal cysteine residue, ET-1 bears remarkable similarities (length and N-terminal -SH) to probes used in our previous nucleic acid sensing strategies[13, 15, 16]. Therefore, we hypothesized that we would be able to functionalize

a. *Department of Pharmaceutical Sciences, Faculty of Pharmacy, University of Toronto, Toronto, ON, Canada, M5S 3M2. Email: shana.kelley@mail.utoronto.ca*
b. *Division of Thoracic Surgery, University of Toronto, Toronto, ON, M5G 1L7*
c. *Latner Thoracic Surgery Research Laboratories, Toronto General Research Institute, University Health Network, Toronto, ON, Canada, M5G 1L7*
d. *Department of Biochemistry, Faculty of Medicine, University of Toronto, Toronto, ON, M5S 3M2, Canada.*

our gold microelectrodes with a synthetic ET-1 self-assembled monolayer (SAM) (Fig. 1c). By introducing an ET-1 specific antibody, we could then measure ET-1 antibodies bound to the electrode surface using an ferrocyanide/ferricyanide electrochemical reporter assay[17]. In brief, a ferrocyanide molecule is sufficiently small to rapidly diffuse to the surface of an modified electrode; however, the presence of a large, blocking protein (ex. ET-1 antibody) can sufficiently impede the diffusion of ferrocyanide to the electrode surface (Figure 1c). As a result, the respective oxidation current of the redox reporter is diminished as shown by signal attenuation during a differential pulse voltammetry (DPV) electrochemical scan. For a description of the electrochemical assay, please refer to the online methods section associated with this work.

In samples collected during EVLP, the presence of the ET-1 peptide in solution would compete with the surface-bound ET-1 for the binding of ET-1 antibodies (Figure 1c, lower track). A portion of the antibody would be bound to solution ET-1 (endogenous levels) and the remaining portion would bind to the synthetic, surface bound ET-1. Thus, we expected to observe changes in ferrocyanide blocking signals due to differential ET-1 antibody levels bound to the electrode surface in the presence of endogenous ET-1. We hypothesized that we could extrapolate the endogenous [ET-1] from the reported values of ET-1 antibodies blocking the electrode surface.

We experimentally validated this scheme by comparing the DPV scans of a sensor with no blocking, complete blocking, and partial blocking due to ET-1 peptide in solution (Fig. 2a). We observed a characteristic attenuation of current in the case of complete blocking (Fig. 2a, dashed line) compared to no blocking (Fig. 2a solid line). As expected, the case where the presence of ET-1 peptide in solution could compete for ET-1 antibodies, we observed only partial blocking (Fig. 2a, dotted line). To confirm that we could quantify the results in Fig. 2a, we then calculated the relative % blocking of an electrode and found approximately 85% blocking with no ET-1 peptide in solution compared to 48% blocking with ET-1 in solution (Fig. 2b). We then titrated the amount of ET-1 antibody detected on the surface of an electrode (Fig. 2c). A titration profile for the signal attenuation as a function of ET-1 antibody concentration was conducted and dynamic range between 0 and 10 ng mL$^{-1}$ of antibody (Fig. 2c) was achieved. Above 10 ng mL$^{-1}$, there was saturation of these sensors. In subsequent proof-of-concept work, we employed sensors that had a higher surface density of synthetic ET-1 peptide (up to 10 μg mL$^{-1}$) to limit the saturation of the sensors thus improving the dynamic range. To further validate this approach, we performed a competitive ET-1 ELISA in parallel to our electrochemical test (Fig. 2d). As expected, we observed a decrease in the OD$_{450nm}$ readings as a result of increasing ET-1 peptide concentration (Fig. 2d). Our ELISA data matched our electrochemical observations, thus validating the approach; however, the time of the electrochemical assay (1.25 hours) was significantly shorter than that of the ET-1 ELISA assay (4 hours).

In order to expand the dynamic range of this approach, we varied the size of each sensor from small to large by changing the

time that the sensors were electrodeposited (30 to 120 seconds) (SI Fig. 1). As expected, the degree to which a sensor was blocked (% available surface) was a product of the electrode size. The largest sensors (120 seconds) exhibited limited antibody concentration dependence followed by the medium (60 seconds) and small (30 seconds) sized sensors (SI Fig. 1). In the case of the smallest sensors (30 seconds), we observed an LOD in the range of 10-100 pg mL$^{-1}$ of ET-1 antibody (SI Fig. 1). Thus, we were able to confirm the ability of the ET-1 assay to be fine-tuned to specific ET-1 peptide levels by altering the size of the biosensing electrodes.

We performed a proof-of-concept study of the ET-1 analysis assay (EAA) (see online methods section), to validate its accuracy. A standard titration of ET-1 antibody concentrations (SI Figure 2, closed circles) was run alongside two samples containing spiked concentrations of ET-1 peptide. From the ET-1 antibody titration, linear regression was used to derive an equation representing the antibody concentration as a function of surface blocking (equation shown in upper left-hand corner of SI Figure 2). From this equation, we then calculated a theoretical antibody concentration from the observed surface blocking effects of the unknown samples ($x_1$ and $x_2$) (dashed line represents the extrapolation curves). By calculating the difference between the concentrations of the known loaded antibody (1 μg mL$^{-1}$) to the experimentally observed antibody concentration, we were able to estimate the solution-based concentration of ET-1 in the samples. Using the EAA approach, we observed an average error of 14% (SI Table 1)). Having met the technical requirements of a specific and rapid peptide detection assay, we sought to biologically validate the ET-1 assay in lung perfusate media.

EVLP perfusate solution, STEEN solution, is an acellular matrix that represents a simplified medium for rapid and sensitive biological analysis. During EVLP, diagnostic biomarkers such ET-1 are present and can accumulate in STEEN solution[2, 18]. Using the same EAA approach as ET-1 detection in PBS, we tested spiked ET-1 levels (500 and 250 ng mL$^{-1}$) in STEEN solution (Figure 3a). We observed ET-1 levels of 526 and 264 ng mL$^{-1}$ respectively resulting in an average error of 5.4% in the spiked STEEN assay for the experimentally derived ET-1 concentrations compared to the actual ET-1 concentrations in solution (Table 1). Thus, we confirmed our ability to successfully extrapolate ET-1 peptide levels in perfusate samples with a high degree of accuracy. To validate this approach in the transplant setting, we then tested perfusate samples collected from a donor lung on EVLP at 3 and 6 hours. Using the EAA, we were able to successfully monitor ET-1 levels over time in lung perfusate during the course of EVLP (Figure 3b). As expected, the integrity of the assay was upheld as the complexity of the sampling matrix was increased from PBS to STEEN. This was anticipated as we observed that the development of a robust SAM on an electrode could provide excellent specificity. Taken together, we were able to demonstrate that the EAA meets the specificity and rapid turnaround parameters required by LTx surgeons to monitor ET-1 peptide levels in lung transplantation-specific media.

In conclusion, we have developed a novel sensing platform capable of detecting very short peptide sequences using a

competitive electrochemical assay. This indirect approach serves as a strong foundation for determining endogenous ET-1 concentrations in lung perfusate and will be of great benefit to transplant teams for the prediction of patient outcomes. Future work will explore efforts that further improve the speed and subsequent timing of the EAA in order to facilitate its clinical implementation. In addition, studies that are focused on determining and quantifying of an absolute cutoff for the ET-1 levels associated with lung and patient outcomes will be investigated. By monitoring ET-1 levels during the transplant process, a new level of biomarker-based patient survival prediction is now possible and this information can be used to guide transplant teams towards targeted therapeutic strategies that, together, will improve the quality of life for the transplant patient.

## Acknowledgements

## References

1. M. Cypel, J. C. Yeung, M. Liu, M. Anraku, F. Chen, W. Karolak, M. Sato, J. Laratta, S. Azad, M. Madonik, C. W. Chow, C. Chaparro, M. Hutcheon, L. G. Singer, A. S. Slutsky, K. Yasufuku, M. de Perrot, A. F. Pierre, T. K. Waddell and S. Keshavjee, *N. Engl. J. Med.*, 2011, **364**, 1431-1440.

2. T. N. Machuca, M. Cypel, Y. Zhao, H. Grasemann, F. Tavasoli, J. C. Yeung, R. Bonato, M. Chen, R. Zamel, Y. M. Chun, Z. Guan, M. de Perrot, T. K. Waddell, M. Liu and S. Keshavjee, *J. Heart Lung Transplant.*, 2015, DOI: 10.1016/j.healun.2015.01.003.

3. A. H. Chester and M. H. Yacoub, *Glob. Cardiol. Sci. Pract.*, 2014, **2014**, 62-78.

4. M. Uguccioni, L. Pulsatelli, B. Grigolo, A. Facchini, L. Fasano, C. Cinti, M. Fabbri, G. Gasbarrini and R. Meliconi, *J. Clin. Pathol.*, 1995, **48**, 330-334.

5. H. Matsumoto, N. Suzuki, H. Onda and M. Fujino, *Biochem. Biophys. Res. Commun.*, 1989, **164**, 74-80.

6. M. E. Ivey, N. Osman and P. J. Little, *Atherosclerosis*, 2008, **199**, 237-247.

7. S. E. Verleden, E. Vandermeulen, D. Ruttens, R. Vos, A. Vaneylen, L. J. Dupont, D. E. Van Raemdonck, B. M. Vanaudenaerde and G. M. Verleden, *Semin. Respir. Crit. Care Med.*, 2013, **34**, 352-360.

8. D. O. Taylor, L. B. Edwards, M. M. Boucek, E. P. Trulock, P. Aurora, J. Christie, F. Dobbels, A. O. Rahmel, B. M. Keck and M. I. Hertz, *J. Heart Lung Transplant.*, 2007, **26**, 769-781.

9. M. Salama, P. Jaksch, O. Andrukhova, S. Taghavi, W. Klepetko and S. Aharinejad, *J. Thorac. Cardiovasc. Surg.*, 2010, **140**, 1422-1427.

10. M. Salama, O. Andrukhova, P. Jaksch, S. Taghavi, W. Kelpetko, G. Dekan and S. Aharinejad, *Transplantation*, 2011, **92**, 155-162.

11. G. I. Snell, M. Rabinov, A. Griffiths, T. Williams, A. Ugoni, R. Salamonsson and D. Esmore, *J. Heart Lung Transplant.*, 1996, **15**, 160-168.

12. B. Lam, J. Das, R. D. Holmes, L. Live, A. Sage, E. H. Sargent and S. O. Kelley, *Nat. Commun.*, 2013, **4**, 2001.

13. B. Lam, Z. Fang, E. H. Sargent and S. O. Kelley, *Anal. Chem.*, 2012, **84**, 21-25.

14. L. Soleymani, Z. Fang, B. Lam, X. Bin, E. Vasilyeva, A. J. Ross, E. H. Sargent and S. O. Kelley, *ACS Nano*, 2011, **5**, 3360-3366.

15. Z. Fang, L. Soleymani, G. Pampalakis, M. Yoshimoto, J. A. Squire, E. H. Sargent and S. O. Kelley, *ACS Nano*, 2009, **3**, 3207-3213.

16. E. Vasilyeva, B. Lam, Z. Fang, M. D. Minden, E. H. Sargent and S. O. Kelley, *Angew. Chem. Int. Ed. Engl.*, 2011, **50**, 4137-4141.

17. J. Das and S. O. Kelley, *Anal Chem*, 2011, **83**, 1167-1172.

18. T. N. Machuca, M. Cypel, J. C. Yeung, R. Bonato, R. Zamel, M. Chen, S. Azad, M. K. Hsin, T. Saito, Z. Guan, T. K. Waddell, M. Liu and S. Keshavjee, *Ann. Surg.*, 2015, **261**, 591-597.
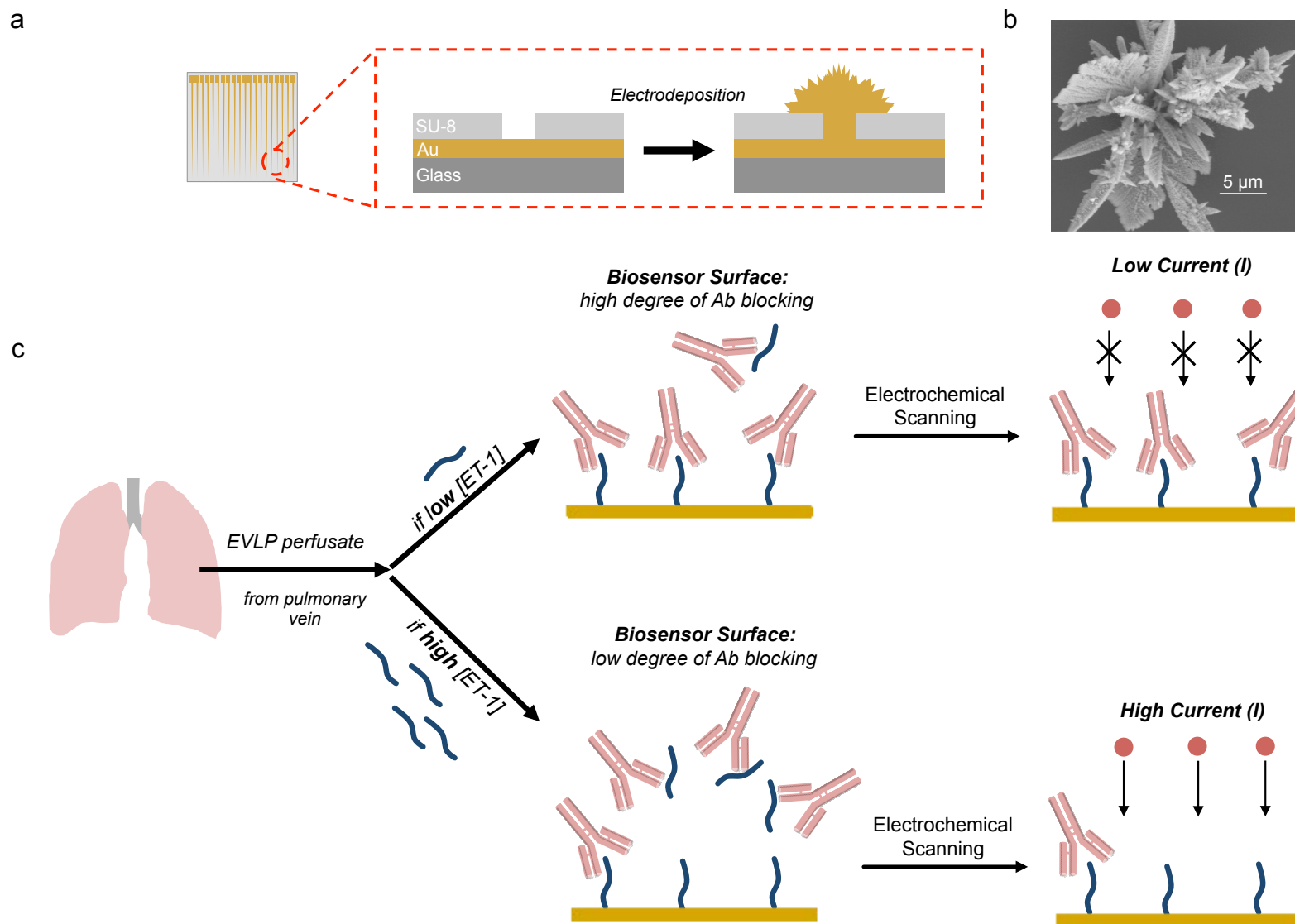
**Figure 1. ET-1 analysis assay (EAA).** (a) Schematic representation of the EAA microchip showing the cross-sectional components of the microchip (dashed red box).  A thin layer of gold is deposited on a glass substrate and passivated with SU-8 using photolithography to create gold apertures for sensor electrodeposition.  (b) An SEM image of an electrodeposited sensor. The scale bar is indicated in the lower right corner of the image. (c) Sensors (yellow) are functionalized via the N-terminal cysteine residue of the ET-1 peptide (blue).  With low levels of ET-1 peptide present in EVLP perfusate (upper track), the addition of ET-1 antibodies (pink) bind and sterically hinder the electrode surface during the oxidation of ferrocyanide (red). Conversely, high levels of endogenous ET-1 in EVLP perfusate (lower track) bind ET-1 antibodies that would otherwise bind the ET-1 peptide on the electrode surface, thus reducing the steric hindrance of electron transfer at the electrode surface.
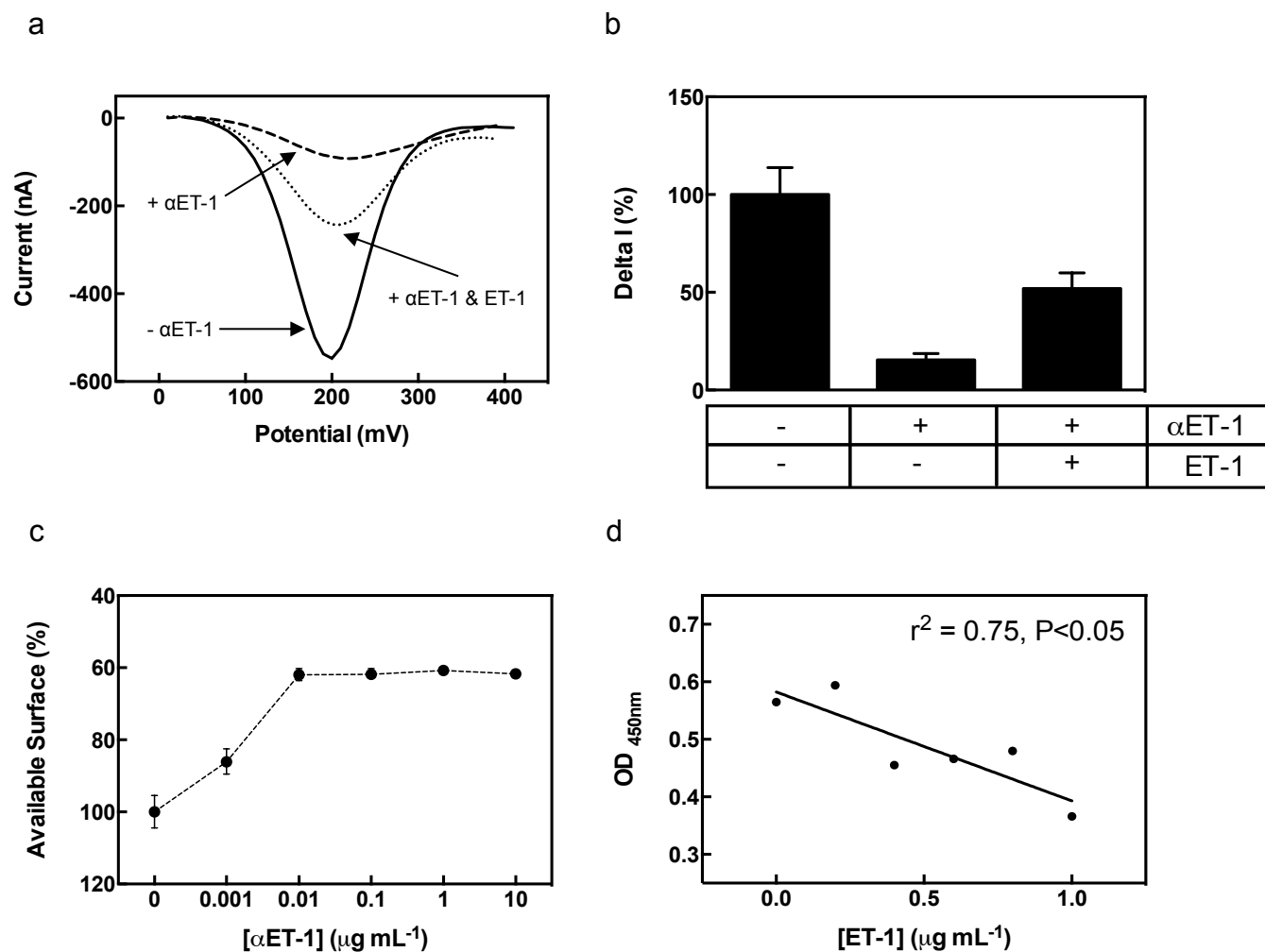
a



b



|   | - | + | + | αET-1 |
|---|---|---|---|---|
|   | - | - | + | ET-1 |

c



d

$r^2 = 0.75$, P<0.05



**Figure 2. Validation of ET-1 detection scheme.** (a) Differential pulse voltammograms for various degrees of sensor blocking arising from: no antibody (solid line), ET-1 antibodies (dashed line), and both ET-1 peptide and antibodies (dotted line) in solution. (b) Representative quantifications of DPV currents with and without antibody or ET-1 peptide present in solution. Each point represents n = 20 different sensors and error-bars indicate s.e.m. (c) Currents obtained (reported as % available surface) for the oxidation of ferrocyanide at the electrode surface for various concentrations of ET-1 antibody bound to ET-1 peptide SAM (1 ng mL⁻¹). Each point represents n = 20 different sensors and error-bars indicate s.e.m. (d) OD 450 nm measurements for various concentrations of endogenous ET-1 using the competitive ELISA-based technique. $r^2$ represents the goodness of fit using non-linear regression. The concentration of ET-1 antibody was1 µg mL⁻¹.
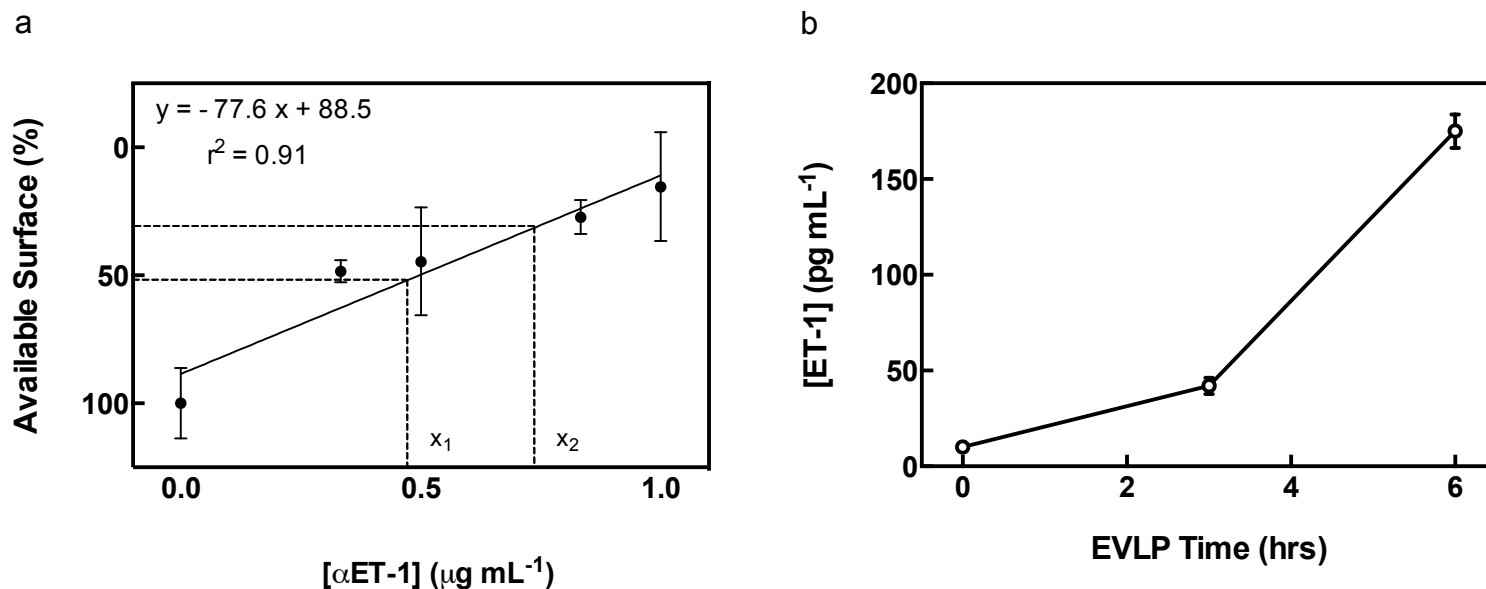
a

$y = -77.6\,x + 88.5$

$r^2 = 0.91$



b



**Figure 3. ET-1 detection in EVLP.** (a) Currents obtained (reported as % available surface) for the oxidation of ferrocyanide at the electrode surface for the detection of ET-1 in STEEN solution. The equation and goodness of fit for the standard curve (circles, solid line) are shown in the upper left quadrant of the graph. Each point represents n = 5 different sensors and error-bars indicate s.e.m. The dashed lines represent the observed % available surface for two spiked ET-1 concentrations, $x_1$ and $x_2$, extrapolated to theoretical anti-ET-1 concentrations. (b) Calculated ET-1 concentrations using the EAA in perfusate samples collected from a donor lung during EVLP. Each point represents n > 3 sensors and error-bars indicate s.e.m.

## Table 1. ET-1 detection for EVLP.

| Buffer | Unknown Sample | % Available Surface | [αET-1] Calculated (ng mL$^{-1}$) | [ET-1] Calculated (ng mL$^{-1}$)* | [ET-1] Actual (ng mL$^{-1}$) |
|---|---|---|---|---|---|
| STEEN | $x_1$ | 52 | 474 | 526 | 500 |
| | $x_2$ | 31 | 736 | 264 | 250 |

*Calculated [ET-1] is obtained from the following equation: [ET-1]calc. = [αET-1] added – [αET-1] calculated where [αET-1] added is 1 μg mL$^{-1}$ and [αET-1] calculated is obtained by solving the equation of the line in Fig. 3a.